Life Sciences 221 (2019) 152–158

Contents lists available at ScienceDirect

Life Sciences

journal homepage: www.elsevier.com/locate/lifescie

Ginsenoside Rg1 protects human retinal pigment epithelial ARPE-19 cells from toxicity of high glucose by up-regulation of miR-26a

Qianqian Shi[a], Xiuying Chen[b], Guangli Sun[c], Lili Wang[d], Longjiang Cui[a,*]

[a] Department of Ophthalmology, Henan Eye Institute, Henan Eye Hospital, Henan Provincial People's Hospital, Zhengzhou 450003, China
[b] Key Laboratory of Advanced Drug Preparation Technologies, Ministry of Education of China, Co-innovation Center of Henan Province for New Drug R&D and Preclinical Safety, School of Pharmaceutical Sciences, Zhengzhou University, Zhengzhou 450000, China
[c] Department of Ophthalmology, The First Affiliated Hospital of Zhengzhou University, Zhengzhou 450000, China
[d] Department of Ophthalmology, People's Hospital of Zhengzhou, Zhengzhou 450000, China

ARTICLE INFO

Keywords:
Diabetic retinopathy
High glucose
Ginsenoside Rg1
microRNA-26a
ERK/Wnt/β-catenin

ABSTRACT

Aims: The therapeutic strategies for diabetic retinopathy (DR) are disappointing. Ginsenoside Rg1 (Rg1) extracted from *Panax ginseng* can induce glucose uptake and lower oxidative stress. We aimed to explore the effect of Rg1 on DR using human retinal pigment epithelium cells (ARPE-19).

Main methods: ARPE-19 cells were grown in high glucose (HG) to simulate DR. Cell viability, apoptosis, ROS generation and miR-26a level were examined by CCK-8 assay, flow cytometry assay, DCFH-DA staining and RT-qPCR, respectively. Expression of proteins associated with viability, apoptosis and oxidative stress was measured by Western blot analysis. Effects of Rg1 on HG-induced alteration were assessed. Moreover, whether miR-26a was involved in Rg1-associated modulation was verified. Finally, the involvements of the ERK and Wnt/β-catenin pathways were analyzed by Western blot analysis.

Key findings: HG reduced cell viability while promoted apoptosis and oxidative stress in ARPE-19 cells. Rg1 ameliorated HG-induced cell injury. The expression of miR-26a was up-regulated by Rg1 in HG-treated cells, and miR-26a inhibition obviously reversed the effects of Rg1 on HG-treated cells. Finally, we found the ERK and Wnt/β-catenin pathways were inhibited by Rg1 through up-regulation of miR-26a.

Significance: Rg1 protected ARPE-19 cells against HG-induced injury through up-regulating miR-26a, along with inhibition of the ERK and Wnt/β-catenin pathways. Rg1 might be a potential therapeutic drug for DR.

1. Introduction

Diabetic retinopathy (DR), the most common microvascular complication of both type 1 and type 2 diabetes, is a burgeoning problem globally [1]. Nonproliferative DR and proliferative DR are the two broad categories of DR with different manifestations, and diabetic macular edema (the most common cause of vision loss) is an additional categorization that occurs across all DR severity levels [1,2]. As the major cause of vision loss in adults, DR leads to capillary, vascular hyperpermeability and neovascularization in the retinal vasculature, and has been estimated to trouble over 95 million people worldwide in 2010 [3,4]. Despite of the extensive studies on the aetiology and pathology of DR, the therapeutic strategies for DR remain disappointing [2]. Further research is warranted on the innovative drugs and therapeutic targets to improve the prognosis of DR.

Retinal pigment epithelium (RPE) is a unique epithelial cell which interacts with photoreceptors and is pivotal for maintaining of normal vision [5]. RPE cells play a crucial role in the pathologic process of DR. High glucose (HG), the result of uncontrolled diabetes, has been reported to induce several retinal microvascular changes, for instance, vascular cell loss and increased extravasation [6,7]. HG may also disrupt the normal functioning of RPE. In DR, biochemical changes may cause retinal damage, and the overproduction of reactive oxygen species (ROS) is considered as a rational explanation for the HG-induced biochemical abnormalities [8]. Moreover, persistent oxidative stress appears to be an important factor underlying the complications of DR [9]. Therefore, the alteration of cell viability, apoptosis and oxidative stress in HG-treated RPE cells is of great importance for the therapy of DR.

Ginsenoside is the major compound extracted from *Panax ginseng*, the most famous herbal medicine in China [10]. There are more than 30 subtypes in ginsenoside family, and all ginsenosides are proven to have

* Corresponding author at: Department of Ophthalmology, Henan Eye Institute, Henan Eye Hospital, Henan Provincial People's Hospital, No.7 Weiwu Road, Zhengzhou 450003, China.
E-mail address: cuilongjiang0021@sina.com (L. Cui).

https://doi.org/10.1016/j.lfs.2019.02.021
Received 7 September 2018; Received in revised form 1 February 2019; Accepted 9 February 2019
Available online 11 February 2019
0024-3205/

broad biological and physiological activities including anti-oxidant and anti-diabetic activities [11,12]. As a valuable pharmacological active triterpene saponin, Ginsenoside Rg1 (Rg1) has been reported to protect mice against cisplation-induced hepatic injury because of the anti-oxidant activities [13]. Previous studies have also proposed that Rg1 induces glucose uptake and lowers oxidative stress in rat skeletal muscles [14,15]. Hence, we hypothesized that Rg1 might be a potential drug to alleviate HG-induced dysfunction of RPE cells. However, the underlying molecular mechanism of Rg1 in protection of RPE cells against HG-induced injury remains unclear.

In this study, we added D-glucose in the culture medium of human RPE cells (ARPE-19) to construct DR model. The effects of Rg1 on cell viability, apoptosis, oxidative stress and possibly associated proteins in HG-treated ARPE-19 cells were studied. The correlation between Rg1 and microRNAs (miRs), the small non-coding RNAs, has been reported previously [16]. Therefore, we further investigated the regulatory mechanism of Rg1 in HG-treated ARPE-19 cells focusing on the downstream miRs. Moreover, the possibly involved signaling pathways were also studied.

2. Materials and methods

2.1. Cell culture and treatment

Human RPE cell line, ARPE-19 (ATCC® CRL-2302™), was obtained from American Type Culture Collection (ATCC; Manassas, VA, USA). As suggested by the manufacturer, the complete culture medium for ARPE-19 cells was consist of Dulbecco's modified Eagle's medium (DMEM)/F-12 (volumetric ratio of 1:1; Hyclone, Logan, UT, USA) and 10% (v/v) heat-inactivated fetal bovine serum (FBS; Hyclone). ARPE-19 cells were cultured in a humidified incubator at 37 °C with 5% CO_2. The culture medium was renewed every other day. Cells at passages 10–15 were used in our study.

For HG treatment, ARPE-19 cells were grown in complete culture medium until 70–80% confluent, and then the culture medium was replaced by FBS-free DMEM/F-12 for 24 h before switching to HG treatment (D-glucose, Sigma-Aldrich, St. Louis, MO, USA). The concentration of D-glucose was 25, 50, 75, 100 or 125 mM. Cells were then incubated at 37 °C for 48 h.

Ginsenoside Rg1 (Rg1; purity ≥ 98%) was purchased from Solarbio (Beijing, China). ARPE-19 cells were pre-treated with Rg1 for 30 min before HG treatment [17].

2.2. Transfection with miRNAs

miR-26a inhibitor and its negative control (NC), synthesized by GenePharma Co. (Shanghai, China), were transfected into ARPE-19 cells, respectively, with the help of Lipofectamine 3000 reagent (Invitrogen, Carlsbad, CA, USA) following the manufacturer's protocol.

2.3. Cell viability assay

The Cell Counting Kit-8 (CCK-8), obtained from Dojindo Molecular Technologies (Kumamoto, Japan), was utilized for measurement of cell viability. In brief, cells were seeded in 96-well plates at 5×10^3 cells/well. After treatment with HG and/or Rg1, 10 μL of CCK-8 solution was added to the culture medium. Then, the 96-well plates were subjected to a humidified incubator at 37 °C for 1 h. The absorbance of each well of these 96-well plates at 450 nm was detected using a Microplate Reader (Bio-Rad, Hercules, CA, USA).

2.4. Apoptosis assay

The Annexin V-FITC Apoptosis Detection Kit (Solarbio) was utilized for identification and quantification of the apoptotic cells. In brief, cells were seeded in 6-well plates at 1×10^5 cells/well. After treatment with HG and/or Rg1, adherent and floating cells were collected and washed twice with cold phosphate buffered saline (PBS; Sigma-Aldrich). Then, cells were resuspended in Binding Buffer (1×10^5 cells per 100 μL) and were stained by 5 μL Annexin V-FITC and 5 μL propidium iodide (PI) at room temperature in the dark. After addition of 500 μL PBS, stained cells were detected by a flow cytometer (Beckman Coulter, Miami, FL, USA), and the percentage of apoptotic cells was analyzed by using FlowJo software (Tree Star, San Carlos, CA, USA).

2.5. Measurement of ROS level

The ROS Assay Kit was utilized for measurement of ROS level. In brief, cells were seeded in 6-well plates at 1×10^5 cells/well. After treatment with HG and/or Rg1, cells were washed twice with cold PBS, followed by incubation in FBS-free culture medium containing 10 μM 2,7-dichlorofluorescein diacetate (DCFH-DA; Nanjing Jiancheng, Nanjing, China) for 30 min. Then, cells were collected and washed with PBS. Afterwards, cells were suspended in 500 μL PBS and the fluorescent intensity was measured using a flow cytometer (488 nm excitation, 521 nm emission).

2.6. Reverse transcription-quantitative PCR (RT-qPCR)

After treatments, total RNA from ARPE-19 cells was isolated using RNAiso Plus (TaKaRa, Dalian, China), as suggested by the manufacturer. The concentration and purity were analyzed by the A260/A280 ratio. Then, 500 ng RNA was subjected to cDNA synthesis with the Taqman MicroRNA Reverse Transcription Kit (Applied Biosystems, Foster City, CA, USA) according to the manufacturer's protocol. The thermocycling program of reverse transcription was 30 min at 16 °C, 30 min at 42 °C and 5 min at 85 °C. Real-time PCR was performed using the Taqman Universal Master Mix II (Applied Biosystems) according to the suggested procedure. The amplification protocol was consisted of an initial denaturation at 95 °C for 10 min, followed by 40 cycles of 95 °C for 15 s and 60 °C for 1 min. The specificity of PCR products was analyzed according to the melting curves. The $2^{-\Delta\Delta Ct}$ method [18] was used for calculation of relative miR-26a expression, which was normalized to U6.

2.7. Western blot analysis

After treatments, ARPE-19 cells were lysed in RIPA buffer (Beyotime, Shanghai, China). Lysates were centrifuged at 15,000 ×*g* at 4 °C for 10 min, and the protein concentration of the supernatant was assessed using the BCA™ Protein Assay Kit (Pierce, Appleton, WI, USA). Protein samples were separated with SDS-PAGE, and proteins in the gels were transferred to polyvinylidene difluoride (PVDF) membranes, followed by blockage of unspecific binding sites using 5% bovine serum albumin (BSA) for 1 h at room temperature. Afterwards, membranes were incubated with primary antibodies against pro poly (ADP)-ribose polymerase (pro PARP; ab194586), cleaved PARP (ab4830), pro caspase-3 (ab90437), cleaved caspase-3 (ab2302), pro caspase-9 (ab32539), cleaved caspase-9 (ab2324), p53 (ab131442), p21 (ab109520), inducible NO synthase (iNOS; ab3523), total (t)-ERK1/2 (ab17942), phospho (p)-ERK1/2 (ab214362), Wnt3a (ab28472), β-catenin (ab32572) or β-actin (ab8227, all Abcam, Cambridge, UK) overnight at 4 °C. Subsequently, PVDF membranes were incubated with horseradish peroxidase (HRP)-conjugated goat anti-rabbit IgG antibody (ab205718) for 1 h at room temperature. Finally, the proteins in the PVDF membranes were visualized by using the ECL reagent (Pierce). The intensity of bands was quantified using ImageJ software (National Institutes of Health, Bethesda, MA, USA).

2.8. Statistical analysis

Statistical analysis was performed using Graphpad Prism 5 software

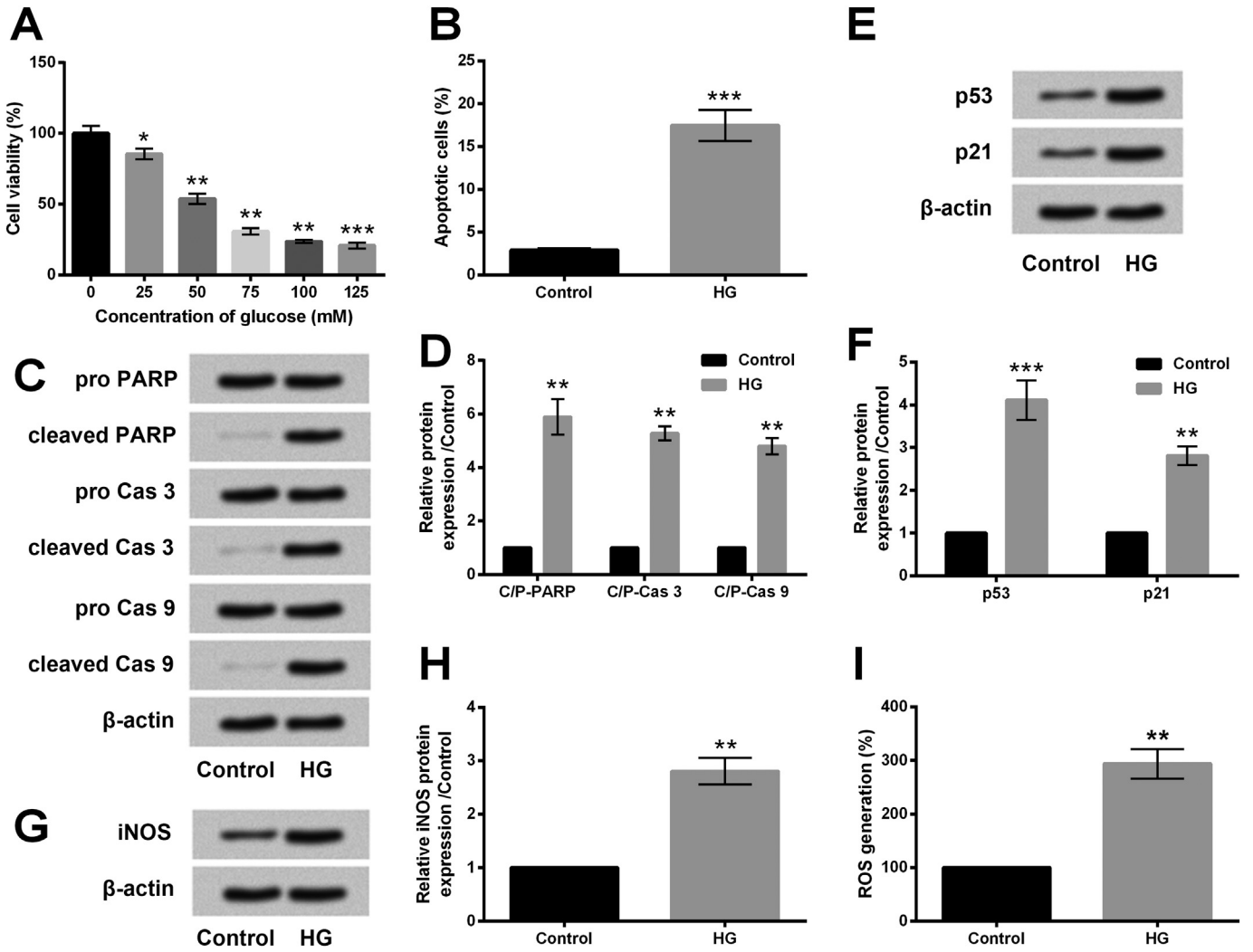

Fig. 1. High glucose (HG) induced ARPE-19 cell injury. ARPE-19 cells were stimulated with a series concentrations of D-glucose (25, 50, 75, 100 and 125 mM) for 48 h, and untreated cells were acted as control. (A) Cell viability was assessed by CCK-8 assay. Cells were treated with 50 mM D-glucose for 48 h, and untreated cells were acted as control. (B) Percentage of apoptotic cells was determined by flow cytometry. (C–D) Expression of proteins associated with apoptosis was evaluated by Western blot analysis. Expression of p53, p21 (E–F) and iNOS (G–H) was assessed by Western blot analysis. (I) ROS level was determined by staining with DCFH-DA. Data presented are the mean ± SD of three independent experiments. *, $P < 0.05$; **, $P < 0.01$; ***, $P < 0.001$. Cas, caspase-; C/P-, cleaved/pro.

(GraphPad, San Diego, CA, USA). Data were presented as the mean ± standard deviation (SD) of three independent experiments. The *P*-values were calculated using the one-way analysis of variance (ANOVA), Student's *t*-test or multiple *t*-tests. Statistical significance was set at $P < 0.05$.

3. Results

3.1. HG induced ARPE-19 cell injury

Cell injury was evaluated according to the alteration of cell viability, apoptosis, ROS level and expression of related proteins. As shown in Fig. 1A, cell viability was significantly reduced after stimulation of 25 mM glucose ($P < 0.05$), 50–100 mM glucose ($P < 0.01$) and 125 mM glucose ($P < 0.001$). Since the cell viability was dropped by half when the dosage of glucose was 50 mM, cells under HG treatment were stimulated with 50 mM glucose. In Fig. 1B, percentage of apoptotic cells after HG stimulation was dramatically higher than the control group ($P < 0.001$). Likewise, HG induced marked increases of cleaved/pro PARP, cleaved/pro caspase-3 and cleaved/pro caspase-9 (all $P < 0.01$, Fig. 1C–D), which was consistent with the results of apoptotic cells. Meanwhile, expression of p53 and p21 was remarkably up-regulated by HG treatment compared with the control group ($P < 0.01$ or $P < 0.001$, Fig. 1E–F). In Fig. 1G–H, HG induced significant up-regulation of iNOS compared with the control group ($P < 0.01$). Besides, we also found the ROS level in HG-treated cells was obviously higher than the control group ($P < 0.01$). Those results described above illustrated that HG induced cell injury of ARPE-19 cells.

3.2. Rg1 ameliorated HG-induced cell injury of ARPE-19 cells

Then, we assessed the effects of Rg1 on HG-treated ARPE-19 cells. Compared with HG-treated cells, cell viability was observably increased by 100–400 μg/mL Rg1 ($P < 0.05$ or $P < 0.01$, Fig. 2A). According to the results of cell viability, cells were stimulated with 100 μg/mL Rg1 in subsequent experiments. Following results showed Rg1 significantly decreased percentage of apoptotic cells ($P < 0.05$, Fig. 2B), lowered the levels of cleaved/pro PARP, cleaved/pro caspase-3 and cleaved/pro caspase-9 (all $P < 0.05$, Fig. 2C–D), and down-regulated the expression of p53, p21 and iNOS (all $P < 0.05$, Fig. 2E–H), when compared with the HG group. Results in Fig. 2I also showed that Rg1 markedly reduced ROS level relative to the HG-treated cells ($P < 0.05$). Those results collectively reflected that Rg1 alleviated HG-induced alterations

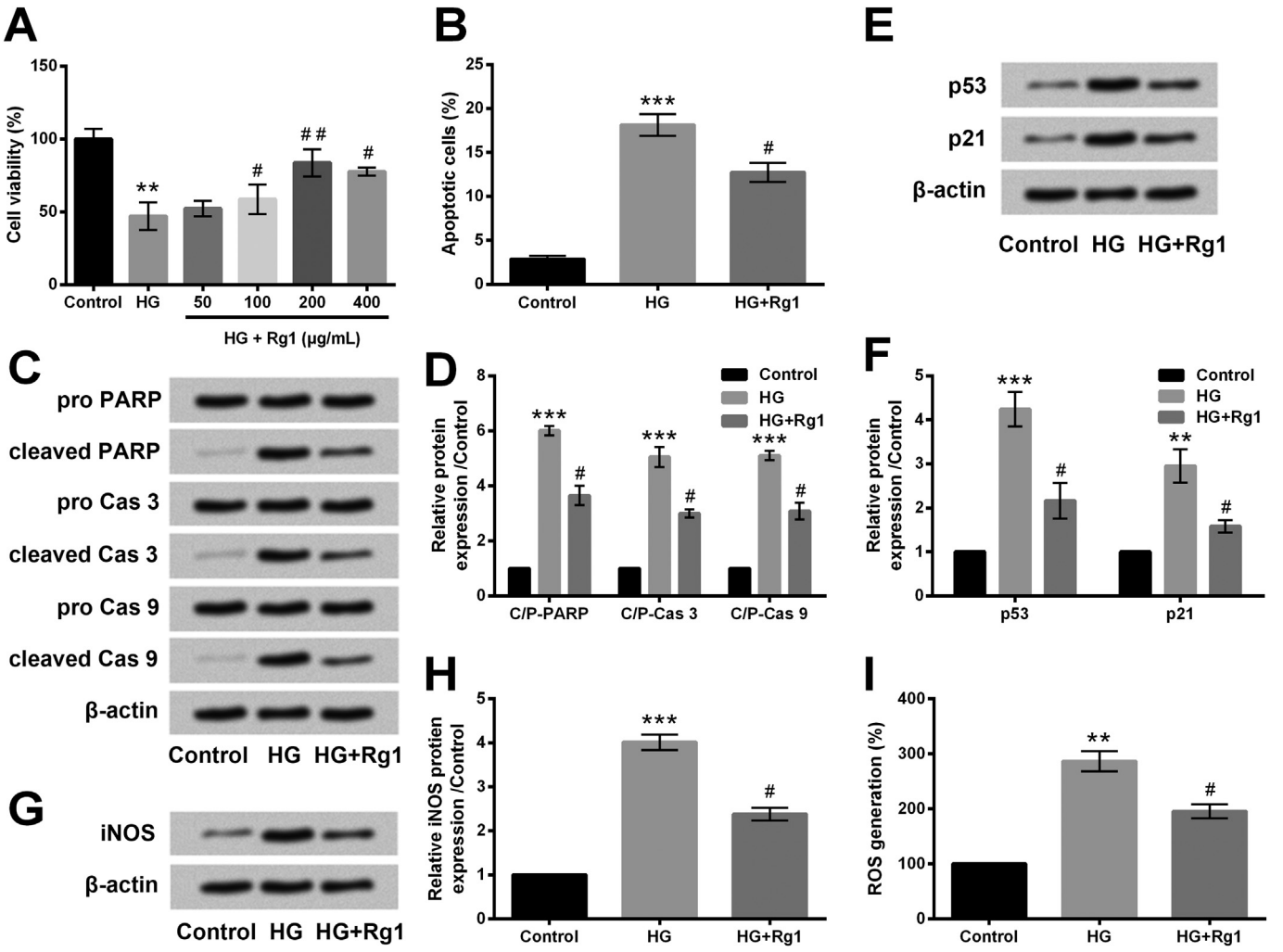

Fig. 2. Ginsenoside Rg1 (Rg1) attenuated high glucose (HG)-induced ARPE-19 cell injury. ARPE-19 cells were stimulated with a series concentrations of Rg1 (0, 50, 100, 200 and 400 μg/mL) for 30 min prior to stimulation of D-glucose (50 mM, 48 h). Untreated cells were acted as control. (A) Cell viability was assessed by CCK-8 assay. ARPE-19 cells were stimulated with Rg1 (0 or 100 μg/mL, 30 min) prior to stimulation of D-glucose (50 mM, 48 h). Untreated cells were acted as control. (B) Percentage of apoptotic cells was determined by flow cytometry. (C–D) Expression of proteins associated with apoptosis was evaluated by Western blot analysis. Expression of p53, p21 (E–F) and iNOS (G-H) was assessed by Western blot analysis. (I) ROS level was determined by staining with DCFH-DA. Data presented are the mean ± SD of three independent experiments. * indicates a significant difference compared with the control group. **, $P < 0.01$; ***, $P < 0.001$. # indicates a significant difference compared with the HG group. #, $P < 0.05$; ##, $P < 0.01$. Cas, caspase-; C/P-, cleaved/pro.

in ARPE-19 cells, suggesting a protective effect of Rg1 on HG-induced injury.

3.3. Rg1 up-regulated miR-26a expression in HG-treated ARPE-19 cells

According to the protective role of Rg1 against HG-induced injury, we measured the expression level of miR-26a to explore whether there was a relationship between Rg1 and miR-26a expression. As shown in Fig. 3, HG treatment observably down-regulated the expression of miR-26a relative to the control group ($P < 0.05$), whereas Rg1 significantly up-regulated the expression of miR-26a compared with the HG group ($P < 0.01$). Results suggested that miR-26a might participate in the modulation of Rg1 in ARPE-19 cells under stimulation with HG.

3.4. Rg1 protected ARPE-19 from HG-induced injury through up-regulating miR-26a

To explore whether miR-26a was involved in the protective effects of Rg1, miR-26a was aberrantly expressed in ARPE-19 cells. Results of RT-qPCR showed miR-26a level in cells transfected with miR-26a inhibitor was prominently lower than the NC-transfected cells ($P < 0.01$,

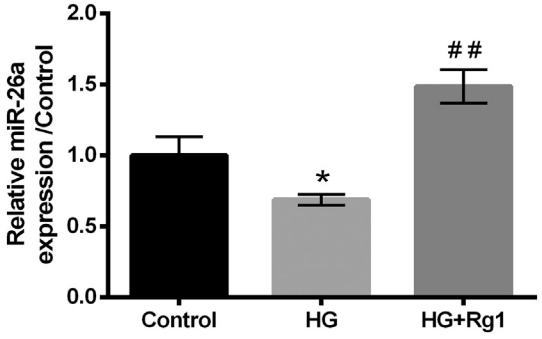

Fig. 3. Ginsenoside Rg1 (Rg1) up-regulated miR-26a expression in high glucose (HG)-treated ARPE-19 cells. ARPE-19 cells were stimulated with Rg1 (0 or 100 μg/mL, 30 min) prior to stimulation of D-glucose (50 mM, 48 h). Untreated cells were acted as control. Expression of miR-26a was determined by RT-qPCR. Data presented are the mean ± SD of three independent experiments. * indicates a significant difference compared with the control group. *, $P < 0.05$. # indicates a significant difference compared with the HG group. ##, $P < 0.01$.

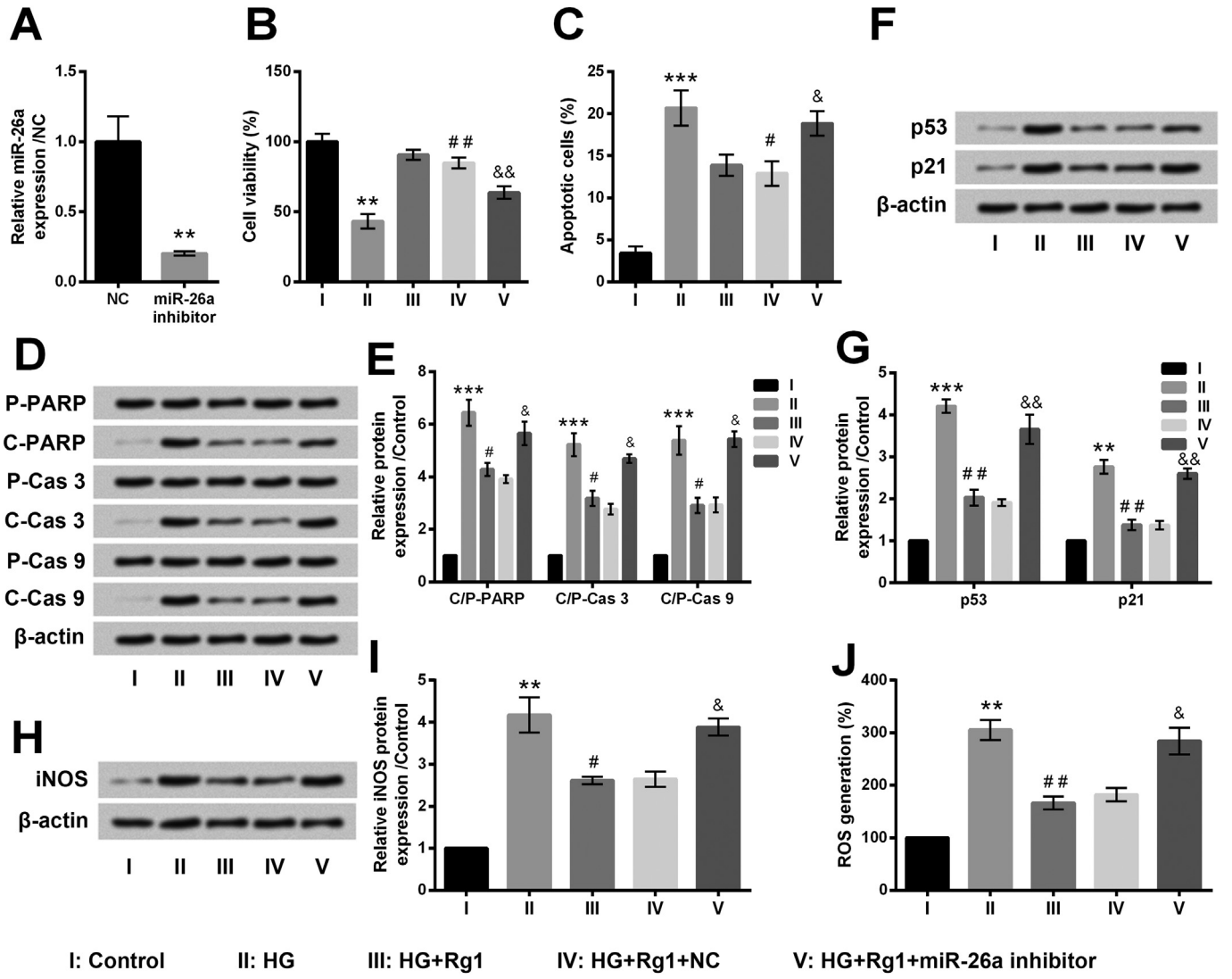

Fig. 4. Ginsenoside Rg1 (Rg1) affected high glucose (HG)-treated ARPE-19 cells through up-regulating miR-26a. ARPE-19 cells were transfected with miR-26a inhibitor or its negative control (NC). (A) Expression of miR-26a was determined by RT-qPCR. Transfected cells were stimulated with Rg1 (100 μg/mL, 30 min) prior to stimulation of D-glucose (50 mM, 48 h). Untransfected cells were stimulated with D-glucose (50 mM, 48 h), and untreated cells were acted as control. (B) Cell viability was assessed by CCK-8 assay. (C) Percentage of apoptotic cells was determined by flow cytometry. (D–E) Expression of proteins associated with apoptosis was evaluated by Western blot analysis. Expression of p53, p21 (F–G) and iNOS (H–I) was assessed by Western blot analysis. (J) ROS level was determined by staining with DCFH-DA. Data presented are the mean ± SD of three independent experiments. * indicates a significant difference compared with the NC group or control group. **, $P < 0.01$; ***, $P < 0.001$. # indicates a significant difference compared with the HG group. #, $P < 0.05$; ##, $P < 0.01$. & indicates a significant difference compared with the HG + Rg1 + NC group. &, $P < 0.05$; &&, $P < 0.01$. Cas, caspase-; P, pro; C, cleaved; C/P-, cleaved/pro.

Fig. 4A), suggesting that miR-26a was knocked down successfully after cell transfection. Then, transfected and untransfected cells were stimulated with HG and/or Rg1. Results showed miR-26a inhibition reversed the effects of Rg1 on HG-treated cells, as miR-26a inhibition significantly reduced cell viability ($P < 0.01$, Fig. 4B), elevated percentage of apoptotic cells ($P < 0.05$, Fig. 4C), increased levels of cleaved/pro PARP, cleaved/pro caspase-3 and cleaved/pro caspase-9 (all $P < 0.05$, Fig. 4D–E), up-regulated expression of p53, p21 and iNOS ($P < 0.05$ or $P < 0.01$, Fig. 4F–I), and enhanced ROS level ($P < 0.05$, Fig. 4J), when compared with the HG + Rg1 + NC group. Those results collectively illustrated that Rg1 might attenuate HG-induced cell injury through up-regulating miR-26a expression in ARPE-19 cells.

3.5. Rg1 inhibited the ERK and Wnt/β-catenin pathways through up-regulating miR-26a

Finally, we studied the possibly involved signaling cascades. On the basis of the results in Fig. 5A–B, phosphorylation levels of ERK1/2 as well as expression levels of Wnt3a and β-catenin were dramatically enhanced by HG treatments ($P < 0.01$ or $P < 0.001$). Meanwhile, Rg1 markedly mitigated the levels of p/t-ERK1/2, Wnt3a and β-catenin ($P < 0.05$ or $P < 0.01$), whereas the effects of Rg1 were significantly reversed by miR-26a inhibition (all $P < 0.05$). Western blot results suggested that Rg1 might inhibit the ERK and Wnt/β-catenin pathways via regulation of miR-26a, which might be a reason for the effects of Rg1 on HG-treated cells.

4. Discussion

Due to the increasing incidence and prevalence of DR worldwide,

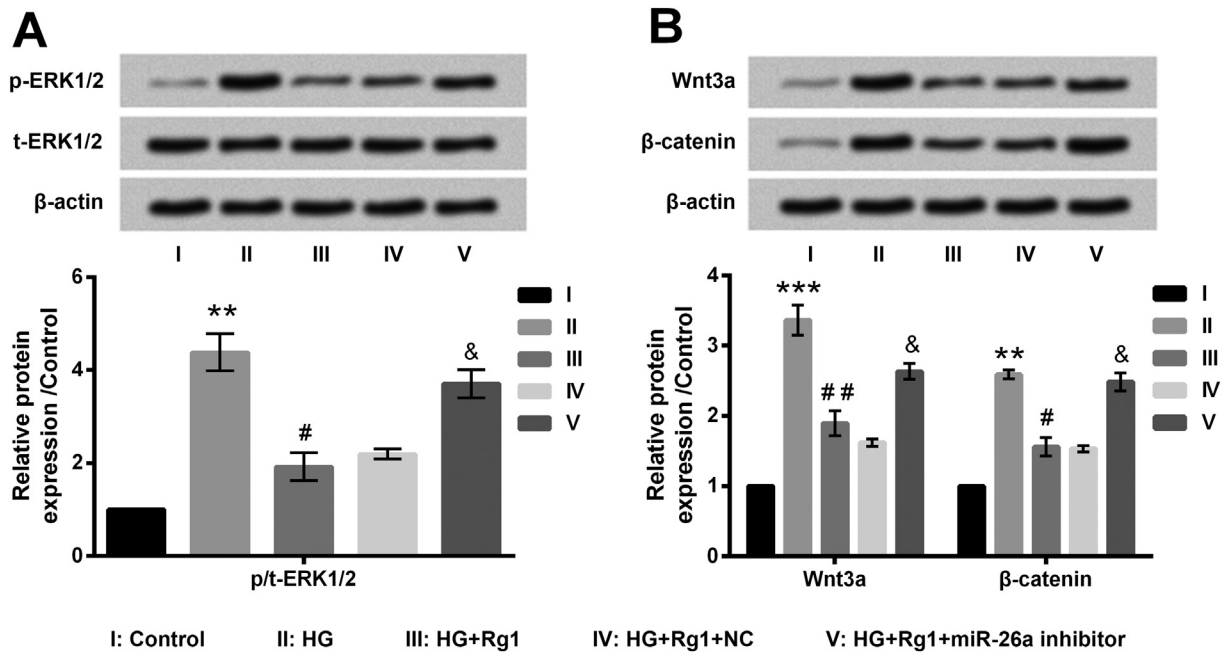

Fig. 5. Ginsenoside Rg1 (Rg1) inhibited the ERK and Wnt/β-catenin pathways via regulation of miR-26a in high glucose (HG)-treated ARPE-19 cells. Transfected ARPE-19 cells were stimulated with Rg1 (100 μg/mL, 30 min) prior to stimulation of D-glucose (50 mM, 48 h). Untransfected cells were stimulated with D-glucose (50 mM, 48 h), and untreated cells were acted as control. Expression of key kinases in the ERK (A) and Wnt/β-catenin (B) was measured by Western blot analysis. Data presented are the mean ± SD of three independent experiments. * indicates a significant difference compared with the control group. **, $P < 0.01$; ***, $P < 0.001$. # indicates a significant difference compared with the HG group. #, $P < 0.05$; ##, $P < 0.01$. & indicates a significant difference compared with the HG + Rg1 + NC group. &, $P < 0.05$. NC, negative control of miR-26a inhibitor.

effective therapeutic drugs as well as the regulatory mechanism become essentially needed. In our study, DR model was constructed in ARPE-19 cells by using HG. We figured out that Rg1 attenuated HG-induced alterations, including decrease of cell viability, increase of apoptotic cells, up-regulation of active PARP, caspase-3, caspase-9, p53, p21, iNOS, and enhancements of ROS generation, in ARPE-19 cells. Then, we provided evidence to prove that Rg1 might protect ARPE-19 cells from HG-induced injury through up-regulating miR-26a. Besides, the ERK and Wnt/β-catenin pathways were involved in the modulation of Rg1.

RPE cells are vulnerable to damage in DR, and the DR model in the study by Shi et al. was constructed in ARPE-19 cells using HG [19]. Similarly, in our study, we also simulated DR in ARPE-19 cells which were grown under HG condition. To evaluate HG-induced cell injury, cell viability, apoptosis and the involved proteins were analyzed. Caspase pathway is an important pathway way involved in cell apoptosis. When this pathway is activated, activated caspase-9 can activate caspase-3, followed by cleavage of PARP, resulting in cell death [20]. In our study, HG reduced cell viability and elevated apoptosis along with activation of the caspase pathway, which was consistent with the study by Liu et al. [21]. p53 is a tumor suppresser that affects cell cycle, DNA damage and cell apoptosis [22]. p21 which can be regulated by p53 is an inhibitor of cell cycle [23]. The up-regulation of p53 and p21 after HG stimulation supported the alteration of cell viability and apoptosis. Oxidative stress after HG treatment was evaluated on account of the alteration of iNOS expression and ROS generation. Nitric oxide is associated with the severity of DR, and iNOS is responsible for the excessive synthesis of nitric oxide [24]. In our study, the up-regulation of iNOS and elevation of ROS generation after HG stimulation reflected that HG induced oxidative stress. Those alterations talked above proved that HG induced ARPE-19 cell injury successfully.

The effects of Rg1 on HG-induced alterations were subsequently studied in our study. Results illustrated that Rg1 attenuated HG-induced decrease of cell viability and repressed apoptosis through inhibiting the caspase pathway. The protective role of Rg1 against HG in ARPE-19 cells was consistent with that against cobalt chloride and hypoxia [25]. Expression of p53 and p21 was down-regulated by Rg1, supporting the alteration of cell viability and apoptosis after Rg1 stimulation. The effects of Rg1 on expression of p53 and p21 in HG-treated ARPE-19 cells were consistent with that in human fibroblasts [26]. A large number of literatures have proven the inhibitory effects of Rg1 on oxidative stress [27,28]. Similarly, results in our study also illustrated that Rg1 suppressed oxidative stress through repressing iNOS expression and lowering intracellular ROS levels. Collectively, we could conclude that Rg1 might protect ARPE-19 cells from HG-induced injury.

miRs are a class of endogenous, small, noncoding RNAs that are discovered recently. Currently, more and more studies identified that miRs participated in the regulation of Rg1 in diverse biological process. Kwok et al. have shown that Rg1 induces angiogenesis of endothelial cells through miR-23 [16]. Zheng et al. also reported that up-regulation of miR-494-3p was contributed to the protective role of Rg1 against ischemia in rat bone marrow mesenchymal stem cells [29]. Therefore, we further studied the regulatory mechanism of Rg1 in ARPE-19 cells focusing on the downstream miRs. A previous study has elucidated that miR-26a attenuates apoptosis in bupivacaine injured mouse dorsal root ganglia through repressing PTEN [30]. Moreover, PTEN, a tumor suppressor, was reported to regulate p53 expression and activity in a literature by Freeman et al. [31]. Considering the alteration of p53 expression after Rg1 treatment, we hypothesized that miR-26a might be a causal link between Rg1 and the protective role. Results in our study reported for the first time that HG-induced down-regulation of miR-26a was reversed by Rg1, suggesting that miR-26a might be involved in Rg1-associated modulations. Additional experiments performed in transfected cells indicated that miR-26a inhibition reversed the effects of Rg1 on HG-induced alterations, consolidating that miR-26a might be the downstream miR of Rg1 in HG-treated ARPE-19 cells. The effects of miR-26a on cell viability and apoptosis of ARPE-19 cells were different from that on cancer cells [32], and the difference between normal cells and cancer cells might be a possible explanation, which needs more supporting experiments.

The ERK and Wnt/β-catenin pathways are two pivotal kinase

cascades that participate in regulation of proliferation, survival and apoptosis [33,34]. A previous study has proven that the ERK pathway is activated by HG stimulation in vascular smooth muscle cells [35]. HG-induced activation of the Wnt/β-catenin pathway is proposed to be an explanation for the link between diabetes and cancer in a study described previously [36]. Therefore, we finally studied the alteration of these two signaling pathways in ARPE-19 cells treated with HG and Rg1. Results in our study showed the ERK and Wnt/β-catenin pathways were inhibited by Rg1, and the inhibition was eliminated by miR-26a inhibition.

In summary, we identified that Rg1 protected ARPE-19 cells against HG-induced injury. The positive correlation between Rg1 and miR-26a was firstly reported, and up-regulation of miR-26a contributed to the protective role of Rg1. In addition, the ERK and Wnt/β-catenin pathways were inhibited by Rg1, possibly due to the up-regulation of miR-26a. This study provided evidence for the potential application of Rg1 in therapy of DR, and miR-26a might be a therapeutic target for DR treatment. More supporting evidence from animal experiments should be provided in the future to promote the therapeutic application of Rg1.

5. Conclusions

Rg1 protected ARPE-19 cells against HG-induced injury through up-regulating miR-26a, along with inhibition of the ERK and Wnt/β-catenin pathways. Rg1 might be a potential therapeutic drug for DR.

Acknowledgements

This research did not receive any specific grant from funding agencies in the public, commercial, or not-for-profit sectors.

Conflict of interest statement

The authors declare that there are no conflicts of interest.

Author contributions

Conceived and designed the experiments: Qianqian Shi, Longjiang Cui and Xiuying Chen; Performed the experiments and analyzed the data: Qianqian Shi; Contributed reagents/materials/analysis tools: Guangli Sun; Wrote the manuscript: Qianqian Shi and Longjiang Cui; Revised the manuscript: Lili Wang.

References

[1] E.J. Duh, J.K. Sun, A.W. Stitt, Diabetic retinopathy: current understanding, mechanisms, and treatment strategies, JCI Insight 2 (2017) e93751.
[2] A.W. Stitt, T.M. Curtis, M. Chen, R.J. Medina, G.J. McKay, A. Jenkins, et al., The progress in understanding and treatment of diabetic retinopathy, Prog. Retin. Eye Res. 51 (2016) 156–186.
[3] D.A. Antonetti, R. Klein, T.W. Gardner, Diabetic retinopathy, N. Engl. J. Med. 366 (2012) 1227–1239.
[4] J.W. Yau, S.L. Rogers, R. Kawasaki, E.L. Lamoureux, J.W. Kowalski, T. Bek, et al., Global prevalence and major risk factors of diabetic retinopathy, Diabetes Care 35 (2012) 556–564.
[5] S. Datta, M. Cano, K. Ebrahimi, L. Wang, J.T. Handa, The impact of oxidative stress and inflammation on RPE degeneration in non-neovascular AMD, Prog. Retin. Eye Res. 60 (2017) 201–218.
[6] A. Chronopoulos, K. Trudeau, S. Roy, H. Huang, S.A. Vinores, S. Roy, High glucose-induced altered basement membrane composition and structure increases trans-endothelial permeability: implications for diabetic retinopathy, Curr. Eye Res. 36 (2011) 747–753.
[7] T. Tien, K.F. Barrette, A. Chronopoulos, S. Roy, Effects of high glucose-induced Cx43 downregulation on occludin and ZO-1 expression and tight junction barrier function in retinal endothelial cells, Invest. Ophthalmol. Vis. Sci. 54 (2013) 6518–6525.
[8] J.J. Garcia-Medina, d.-R.-V. Monica, M. Garcia-Medina, V. Zanon-Moreno, R. Gallego-Pinazo, M.D. Pinazo-Duran, Chapter 4 - diabetic retinopathy and oxidative stress, in: V.R. Preedy (Ed.), Diabetes: Oxidative Stress and Dietary Antioxidants, Academic Press, San Diego, 2014, pp. 33–40.
[9] G.A. Lutty, Effects of diabetes on the eye, Invest. Ophthalmol. Vis. Sci. 54 (2013) Orsf81–7.
[10] M. Wang, S.-J. Yan, H.-T. Zhang, N. Li, T. Liu, Y.-L. Zhang, et al., Ginsenoside Rh2 enhances the antitumor immunological response of a melanoma mice model, Oncol. Lett. 13 (2017) 681–685.
[11] Q.F. Gui, Z.R. Xu, K.Y. Xu, Y.M. Yang, The efficacy of ginseng-related therapies in type 2 diabetes mellitus: an updated systematic review and meta-analysis, Medicine (Baltimore) 95 (2016) e2584.
[12] C.R. Hwang, S.H. Lee, G.Y. Jang, I.G. Hwang, H.Y. Kim, K.S. Woo, et al., Changes in ginsenoside compositions and antioxidant activities of hydroponic-cultured ginseng roots and leaves with heating temperature, J. Ginseng Res. 38 (2014) 180–186.
[13] Y. Gao, S. Chu, Q. Shao, M. Zhang, C. Xia, Y. Wang, et al., Antioxidant activities of ginsenoside Rg1 against cisplatin-induced hepatic injury through Nrf2 signaling pathway in mice, Free Radic. Res. 51 (2017) 1–13.
[14] H.M. Lee, O.H. Lee, K.J. Kim, B.Y. Lee, Ginsenoside Rg1 promotes glucose uptake through activated AMPK pathway in insulin-resistant muscle cells, Phytother. Res. 26 (2012) 1017–1022.
[15] S.H. Yu, H.Y. Huang, M. Korivi, M.F. Hsu, C.Y. Huang, C.W. Hou, et al., Oral Rg1 supplementation strengthens antioxidant defense system against exercise-induced oxidative stress in rat skeletal muscles, J. Int. Soc. Sports Nutr. 9 (2012) 23.
[16] H.H. Kwok, L.S. Chan, P.Y. Poon, P.Y. Yue, R.N. Wong, Ginsenoside-Rg1 induces angiogenesis by the inverse regulation of MET tyrosine kinase receptor expression through miR-23a, Toxicol. Appl. Pharmacol. 287 (2015) 276–283.
[17] Q. He, J. Sun, Q. Wang, W. Wang, B. He, Neuroprotective effects of ginsenoside Rg1 against oxygen-glucose deprivation in cultured hippocampal neurons, J. Chin. Med. Assoc. 77 (2014) 142–149.
[18] K.J. Livak, T.D. Schmittgen, Analysis of relative gene expression data using real-time quantitative PCR and the 2(−delta delta C(T)) method, Methods 25 (2001) 402–408.
[19] H. Shi, Z. Zhang, X. Wang, R. Li, W. Hou, W. Bi, et al., Inhibition of autophagy induces IL-1beta release from ARPE-19 cells via ROS mediated NLRP3 inflammasome activation under high glucose stress, Biochem. Biophys. Res. Commun. 463 (2015) 1071–1076.
[20] A. Mondal, L.L. Bennett, Resveratrol enhances the efficacy of sorafenib mediated apoptosis in human breast cancer MCF7 cells through ROS, cell cycle inhibition, caspase 3 and PARP cleavage, Biomed. Pharmacother. 84 (2016) 1906–1914.
[21] W.Y. Liu, S.S. Liou, T.Y. Hong, I.M. Liu, Hesperidin Prevents High Glucose-Induced Damage of Retinal Pigment Epithelial Cells, Planta Med. 84 (2018) 1030–1037.
[22] J. Liu, C. Zhang, W. Hu, Z. Feng, Tumor suppressor p53 and its mutants in cancer metabolism, Cancer Lett. 356 (2015) 197–203.
[23] P. Galanos, K. Vougas, D. Walter, Chronic p53-independent p21 expression causes genomic instability by deregulating replication licensing, 18 (2016) 777–789.
[24] S. Sharma, S. Saxena, K. Srivastav, R.K. Shukla, N. Mishra, C.H. Meyer, et al., Nitric oxide and oxidative stress is associated with severity of diabetic retinopathy and retinal structural alterations, Clin. Exp. Ophthalmol. 43 (2015) 429–436.
[25] K.R. Li, Z.Q. Zhang, J. Yao, Y.X. Zhao, J. Duan, C. Cao, et al., Ginsenoside Rg-1 protects retinal pigment epithelium (RPE) cells from cobalt chloride (CoCl2) and hypoxia assaults, PLoS One 8 (2013) e84171.
[26] B.R. Zhou, Y. Xu, D. Wu, F. Permatasari, Y.Y. Gao, D. Luo, Ginsenoside Rg1 protects human fibroblasts against psoralen- and UVA-induced premature senescence through a telomeric mechanism, Arch. Dermatol. Res. 304 (2012) 223–228.
[27] Y. Wang, Q. Liu, Y. Xu, Y. Zhang, Y. Lv, Y. Tan, et al., Ginsenoside Rg1 protects against oxidative stress-induced neuronal apoptosis through myosin IIA-actin related cytoskeletal reorganization, Int. J. Biol. Sci. 12 (2016) 1341–1356.
[28] G. Zu, J. Guo, N. Che, T. Zhou, X. Zhang, Protective effects of ginsenoside Rg1 on intestinal ischemia/reperfusion injury-induced oxidative stress and apoptosis via activation of the Wnt/beta-catenin pathway, Sci. Rep. 6 (2016) 38480.
[29] H.Z. Zheng, X.K. Fu, J.L. Shang, R.X. Lu, Y.F. Ou, C.L. Chen, Ginsenoside Rg1 protects rat bone marrow mesenchymal stem cells against ischemia induced apoptosis through miR-494-3p and ROCK-1, Eur. J. Pharmacol. 822 (2018) 154–167.
[30] C. Cui, G. Xu, J. Qiu, X. Fan, Up-regulation of miR-26a promotes neurite outgrowth and ameliorates apoptosis by inhibiting PTEN in bupivacaine injured mouse dorsal root ganglia, Cell Biol. Int. 39 (2015) 933–942.
[31] D.J. Freeman, A.G. Li, G. Wei, H.H. Li, N. Kertesz, R. Lesche, et al., PTEN tumor suppressor regulates p53 protein levels and activity through phosphatase-dependent and -independent mechanisms, Cancer Cell 3 (2003) 117–130.
[32] Y. Gong, W. Wu, X. Zou, F. Liu, T. Wei, J. Zhu, MiR-26a inhibits thyroid cancer cell proliferation by targeting ARPP19, Am. J. Cancer Res. 8 (2018) 1030–1039.
[33] C.A. Buckner, A.L. Buckner, S.A. Koren, M.A. Persinger, R.M. Lafrenie, Exposure to a specific time-varying electromagnetic field inhibits cell proliferation via cAMP and ERK signaling in, Cancer Cells 39 (2018) 217–230.
[34] T. Yoshida, N.A. Sopko, M. Kates, X. Liu, G. Joice, D.J. McConkey, et al., Three-dimensional organoid culture reveals involvement of Wnt/β-catenin pathway in proliferation of bladder cancer cells, Oncotarget 9 (2018) 11060–11070.
[35] Y. Liu, X. Li, S. Jiang, Q. Ge, Tetramethylpyrazine protects against high glucose-induced vascular smooth muscle cell injury through inhibiting the phosphorylation of JNK, p38MAPK, and ERK, 46 (2018) 3318–3326.
[36] C. Garcia-Jimenez, J.M. Garcia-Martinez, A. Chocarro-Calvo, A. De la Vieja, A new link between diabetes and cancer: enhanced WNT/beta-catenin signaling by high glucose, J. Mol. Endocrinol. 52 (2014) R51–R66.